Pathology of Head and Neck Tumors

Pathology of Head and Neck Tumors:

Case Studies from Asan Medical Center

By

Kyung-Ja Cho

Cambridge
Scholars
Publishing

Pathology of Head and Neck Tumors:
Case Studies from Asan Medical Center

By Kyung-Ja Cho

This book first published 2024

Cambridge Scholars Publishing

Lady Stephenson Library, Newcastle upon Tyne, NE6 2PA, UK

British Library Cataloguing in Publication Data
A catalogue record for this book is available from the British Library

ISBN (10): 1-0364-0735-7
ISBN (13): 978-1-0364-0735-3

TABLE OF CONTENTS

PREFACE

This book represents the summary of my twenty-four-year tenure as a head and neck pathologist at Asan Medical Center. It endeavors to combine my clinical experience, the intricacies of head and neck tumor statistics in Korea, and valuable insights for Pathology trainees and clinicians specializing in head and neck oncology. The book's dataset encompasses malignant and benign head and neck tumors diagnosed between 2000 and 2020 at Asan Medical Center in Seoul, Korea. Tumors originating from the brain, facial skin and its appendages (excluding the eye and ear), lymph nodes, thyroid gland, and parathyroid gland have been excluded from this dataset.

The methodology employed involved review of pathology materials and medical records, with approval granted by the Asan Medical Center Institutional Review Board (Approval Number: 2022-0911). It's pertinent to mention that recurrent tumors were omitted from statistical analyses, and the enumeration of distinct tumors within individual patients was undertaken. However, the compilation of survival outcomes for the entire patient cohort proved unfeasible.

Numerous pathologists have merited my deep appreciation for their dedication and enthusiasm in diagnosing a diverse array of diseases, including those concerning head and neck tumors. I am equally indebted to the scientists, trainees, and technologists within the Pathology Department, whose collaboration has enriched my professional journey over the years. Respect and gratitude are extended to the esteemed professors at Asan Medical Center's Departments of Otolaryngology, Ophthalmology, Oral & Maxillofacial Surgery, Plastic Surgery, Oncology, Radiology, Radiation Oncology, and Nuclear Medicine, whose trust and support have been encouraging in fostering my Pathology practice.

It is my aspiration that this book not only delineates the prevailing landscape of head and neck tumors in Korea but also highlights the epidemiological disparities from Western nations. Moreover, I anticipate that this work will heighten curiosity and comprehension among medical personnel involved in head and neck oncology.

August, 2023
Kyung-Ja Cho

OVERVIEW

The statistical analysis and categorization of both malignant and benign tumors originating in the head and neck, which were diagnosed at Asan Medical Center (AMC) in Seoul, Korea, spanning the period from 2000 to 2020, are presented in Table 0. The classification schema is established in accordance with the following references: the WHO (World Health Organization) Classification of Head and Neck Tumours, 5th Edition (2022) (available online), the WHO Classification of Tumours of Soft Tissue and Bone, 5th Edition (2020), the WHO Classification of Tumours of the Eye, 5th Edition (2023) (available online), and the WHO Classification of Skin Tumours, 5th Edition (2023) (available online). Squamous intraepithelial neoplasia has not been included in the analysis. Intermediate categories of bone and soft tissue tumors are designated as benign.

The aggregated dataset encompasses a total of 20,066 cases, with malignant tumors accounting for 44% of the total, and benign tumors constituting the remaining 56%. Among the cohort of 19,872 primary tumors, epithelial tumors comprise 65%, while non-epithelial tumors constitute the remaining 35%.

Table 0. Categories of tumors of head and neck diagnosed at Asan Medical Center from 2000 through 2020*

		Malignant	Benign	Total
Epithelial tumors	Squamous cell carcinomas	5,677		5,677
	Salivary gland tumors	1,086	3,281	4,367
	Other tumors	279	2,647	2,926
	Subtotal	7,042	5,928	12,970
Mesenchymal tumors		429	4,613	5,042
Odontogenic tumors		7	354	361
Melanocytic tumors		151	174	325
Neuronal tumors		80	2	82
Neuroendocrine tumors		1	70	71
Germ cell tumors		8	3	11
Lymphoreticular tumors (extranodal)		991	19	1,010
Metastatic tumors (except of lymph node & bone)		194		194
Total		8,903	11,163	20,066

*Tumors of brain, facial skin & skin appendage, lymph node, thyroid and parathyroid gland are excluded.

CHAPTER 1

SQUAMOUS CELL CARCINOMAS

Squamous cell carcinomas constituted 62% of all malignant tumors and 79% of all carcinomas, presenting as the predominant malignant tumor type within the head and neck region. Squamous cell carcinoma (SCC) is characterized by its morphological attributes, including keratin pearls, individual cell keratinization, and intercellular bridges, and it arises not only from squamous epithelium but also from respiratory epithelium or glandular tissue. The conventional classification of SCCs is contingent on the degree of squamous differentiation within the histological framework, as delineated below: well-differentiated SCCs exhibit mild cellular atypia and prominent keratinization; moderately differentiated SCCs manifest moderate cellular atypia and modest keratinization; poorly differentiated SCCs present marked cellular atypia and indistinct squamous differentiation. Variants encompass basaloid, spindle cell, verrucous, and papillary SCC, in addition to non-keratinizing SCC, which should not be conflated with poorly differentiated SCC, primarily occurring in the oropharynx, nasopharynx, and sinonasal tract.

Importantly, it is crucial to acknowledge that the morphological attributes and epidemiological characteristics of head and neck SCCs demonstrate distinct variations specific to individual anatomical sites. This divergence can be attributed to the inherent histological and embryological differences existing among the heterogeneous regions that constitute the head and neck domain.

Table 1-1 provides a comprehensive presentation of statistics pertaining to the subtypes and distribution patterns of head and neck squamous cell carcinomas diagnosed between 2000 and 2020, along with accompanying mean age and gender ratios. The larynx emerges as the most frequently affected site, closely followed by the oral cavity and oropharynx. Within this context, elderly men predominantly comprise the patient population across all sites. However, the mean age and gender ratio manifest site-specific variations. The highest mean age is observed in SCC of the lip (68.8 years), while the lowest mean age is noted in nasopharyngeal SCC (54.1 years). Moreover, the most pronounced male predominance is evident in

SCC of the larynx and hypopharynx (male-to-female ratio ranging from 15.1 to 16.5 : 1), whereas a less pronounced male predominance is observed in SCC of the eye, ear, and sinonasal tract (male-to-female ratio ranging from 1.8 to 2.6 : 1).

Table 1-1. Subtypes and distribution of head and neck squamous cell carcinomas with mean age and gender ratio

Sites Subtypes	Oral cavity	Lip	Oro-pharynx	Larynx	Hypo-pharynx	Sinonasal tract	Naso-pharynx	Salivary gland	Eye & LDS	Ear	UPS	Total
SCC, W/D	690	32	78	404	58	41		2	9	59		1,373
SCC, M/D	487	17	532	800	397	126	43	14	11	26		2,453
SCC, P/D	71	2	248	81	101	68			4	5		580
SCC, NK			16			26	648		1			691
Basaloid SCC	5		12	10	19	4	5	1		2		58
Spindle cell SCC	5		2	11	5	6	1			1		31
VC	14	1		2		1				3		21
Papillary SCC	1		3	1		6						11
SCC, NOS	28	4	125	75	65	10	14	1	2	2	133	459
Total	1,301	56	1,016	1,384	645	288	711	18	27	98	133	5,677
Mean age	58.4	68.8	59.4	64.2	65.4	59.4	54.1	66.1	62.3	63.4	60.2	62.0
Gender ratio (male : female)	2.9 : 1	2.7 : 1	5.7 : 1	16.5 : 1	15.1 : 1	2.6 : 1	3.3 : 1	4.7 : 1	1.8 : 1	2.5: 1	5.7 : 1	5.8 : 1

LDS, lacrimal drainage system; UPS, unknown primary site; SCC, squamous cell carcinoma; W/D, well differentiated; M/D, moderately differentiated; P/D, poorly differentiated; NK, non-keratinizing; VC, verrucous carcinoma; NOS, not otherwise specified

1.1. Squamous cell carcinoma of oral cavity and lip

Statistics pertaining to the subtypes and distribution of oral cavity and lip squamous cell carcinomas (SCCs) are concisely presented in Table 1-2. Among these, the tongue constituted the most prevalent subsite, accounting for 59% of cases (Fig. 1-1). This was succeeded by the buccal mucosa (10%) and the floor of the mouth (9%) in terms of frequency. Some variations in the degree of differentiation based on subsites were discernible, and a substantial majority of oral cavity and lip SCCs, specifically 90%, exhibited histological differentiation that was either well or moderately differentiated.

Table 1-2. Subtypes and distribution of oral cavity and lip squamous cell carcinomas

Subsites / Subtypes	Tongue	Buccal mucosa	Floor of mouth	Gingiva & mandible	Hard palate & maxilla	Retromolar trigone	NOS	Lip	Total
SCC, W/D	448	68	49	59	19	22	25	32	722
SCC, M/D	291	47	60	42	14	17	16	17	504
SCC, P/D	37	14	4	4	4	3	5	2	73
SCC, NOS	14	7	3	2	1	1		4	32
VC	7	2		4			1	1	15
Basaloid SCC			1	2	1	1			5
Spindle cell SCC	1			4					5
Papillary SCC					1				1
Total	798	138	117	117	40	44	47	56	1,357

NOS, not otherwise specified; SCC, squamous cell carcinoma; W/D, well differentiated; M/D, moderately differentiated; P/D, poorly differentiated; VC, verrucous carcinoma

Despite their favorable degree of differentiation, squamous cell carcinomas occurring within the oral cavity exhibit a propensity for a conspicuously infiltrative growth pattern. The 8th edition of the AJCC Cancer Staging Manual introduces the concept of the 'worst pattern of invasion (WPOI)' as a predictive marker for outcomes in patients with oral cavity SCCs. The delineation of WPOI encompasses the following typologies: type 1, characterized by a pushing border; type 2, featuring a finger-like growth pattern; type 3, characterized by large, separate islands comprising more than 15 cells per island; type 4, consisting of small tumor islands comprising 15 cells or fewer per island; and type 5, tumor satellites situated at a distance of ≥1mm from the main tumor or from the nearest neighboring satellite. A complementary prognostic element, namely tumor budding, defined as the presence of four or fewer tumor cells, has also emerged as a notable prognostic factor (Fig. 1-2).

Tobacco and alcohol have traditionally been cited as prototypical risk factors for oral cavity SCC. However, there has been a global increase in the incidence of young, non-smoking patients with oral SCC, a phenomenon we reported in 2019. The current dataset encompasses 167 non-smoking males and 67 non-smoking females under the age of 45 (constituting 17% of the cohort), yet the underlying pathogenesis within this subgroup remains

uncertain.

Human papillomavirus (HPV) is implicated in a subset of oral cavity SCC cases, albeit to a lesser extent compared to its association with oropharynx SCC. The identification of HPV in cancerous tissue can be achieved through techniques such as polymerase chain reaction (PCR), *in situ* hybridization (ISH), or immunohistochemistry (IHC) targeting the p16 protein. p16, a cyclin-dependent kinase inhibitor, is used as a surrogate marker for HPV due to its paradoxical accumulation resulting from the loss of pRb due to the HPV E7 protein. However, it does not completely align with HPV status. In our dataset, 6% of the 175 oral cavity SCC cases tested positive for HPV, and 14% of the 151 cases were found to be p16-positive. HPV types 16 (4 cases), 18 (1 case), 30 (1 case), and other types (3 cases) were detected in male patients aged between 38 and 72 years.

Approximately 10~15% of oral cavity SCC cases are postulated to originate from intraepithelial dysplasia. However, the precise pathological and clinical aspects of this developmental process remain ambiguous, in part due to the lack of clear criteria for defining oral epithelial dysplasia, the considerable inter-observer variability among pathologists, and the loss of follow-up after complete removal of dysplastic lesions.

Proliferative verrucous leukoplakia (PVL) represents a distinctive and infrequent premalignant lesion of the oral mucosa, uniquely characterized by its lack of association with smoking, alcohol, or HPV. PVL is recognized to progress through distinct developmental phases, namely: 1) focal flat white keratosis (Fig. 1-3), 2) the emergence of diffused and multifocal white patches, 3) horizontal and exophytic growth leading to a warty surface appearance, and 4) eventual progression to verrucous carcinoma or squamous cell carcinoma (SCC). Over the period spanning from 2017 to 2020 at AMC, eight cases of PVL were diagnosed, involving three males and five females aged between 51 and 89 years. None of these cases have undergone malignant transformation thus far.

Verrucous carcinoma, a distinct variant of SCC, primarily affects the oral cavity. Histologically, it is characterized by a highly mature squamous epithelium exhibiting upward papillary projections, significant hyperkeratosis, and broad-based downward pushing, while lacking the infiltration of individual tumor cells (Fig. 1-4). Notably, a focal biopsy of this tumor may appear non-malignant upon interpretation. The prognosis associated with verrucous carcinoma is generally more favorable compared to that of conventional SCC due to its non-invasive growth pattern.

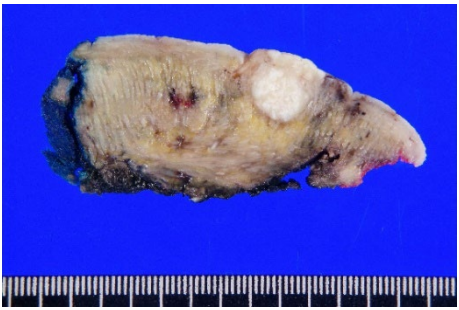

Fig. 1-1. Gross feature of squamous cell carcinoma of the tongue. The cut surface of tumor is solid, whitish, and infiltrative from the surface.

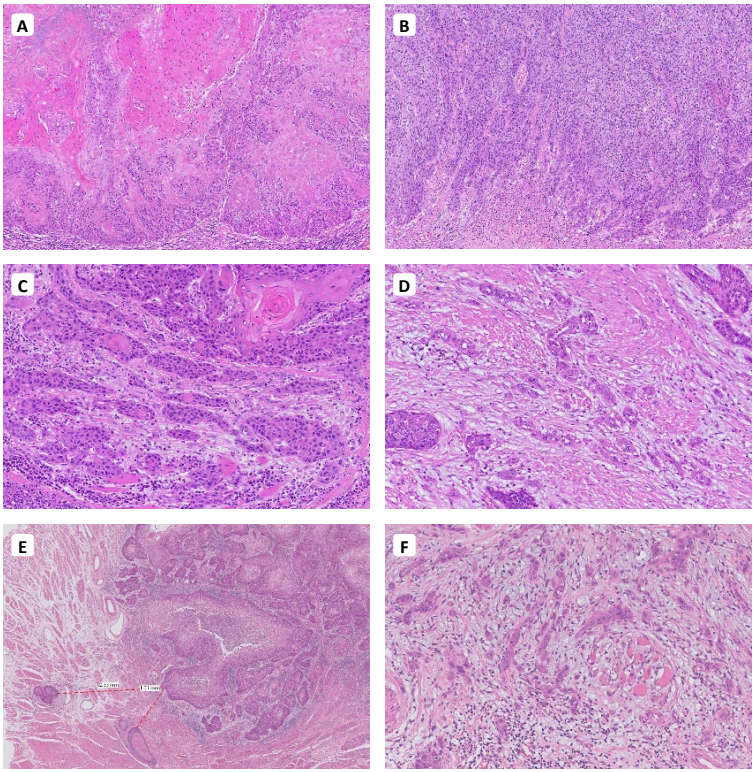

Fig. 1-2. Squamous cell carcinoma of the oral cavity. A. Tumor is well differentiated with keratinization and mild cellular atypia, and shows a pushing border (worst pattern of invasion (WPOI) type 1). B. Tumor is poorly differentiated without

keratinization, and shows finger-like growth (WPOI type 2). C. Tumor is moderately differentiated with cellular atypia and focal keratinization, and shows large separate islands, >15 cells (WPOI type 3). D. There are small tumor islands, ≤15 cells (WPOI type 4). E. There are tumor satellites and perineural invasion ≥1mm from main tumor (WPOI type 5). F. There are tumor buddings ≤4 cells.

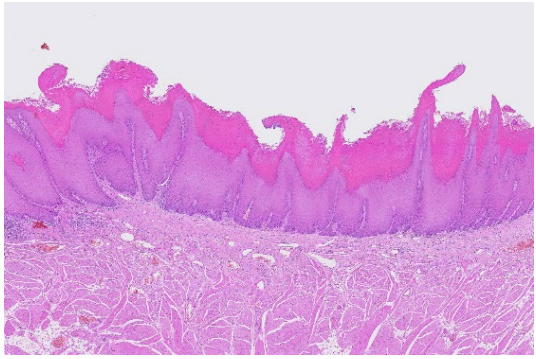

Fig. 1-3. Proliferative verrucous leukoplakia of the oral cavity. Verruciform epithelial hyperplasia is accompanied by hyperkeratosis.

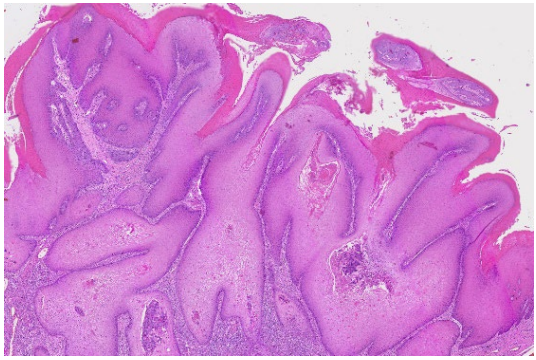

Fig. 1-4. Verrucous carcinoma of the oral cavity. Well differentiated squamous epithelial proliferation is showing a hyperkeratotic verrucous surface and broad downward pushing borders.

1.2. Squamous cell carcinoma of oropharynx

The distribution and subtypes of oropharyngeal squamous cell carcinomas (SCCs) are presented in Table 1-3. The palatine tonsil presented as the predominant subsite, accounting for 69% of cases, followed by the

base of the tongue (18%) and the soft palate (6%). The table provides information regarding the degree of differentiation. However, it is presently recommended to refrain from assigning grades to HPV- or p16-positive oropharyngeal SCCs following testing.

Table 1-3. Subtypes and distribution of oropharyngeal squamous cell carcinomas

Subsites / Subtypes	Palatine tonsil	Base of tongue	Soft palate	Vallecula	PPW	Lateral wall	Tonsillar pillar	Uvula	NOS	Total
SCC, W/D	35	17	21	1	2		2			78
SCC, M/D	369	97	26	12	8	6	4	6	4	532
SCC, P/D	188	40	9	3	3	2	1	1	1	248
SCC, NK	13	2	1							16
SCC, NOS	83	26	6	1		1			8	125
Basaloid SCC	7	3		1		1				12
Papillary SCC	3									3
Spindle cell SCC	1				1					2
Total	699	185	63	18	14	10	7	7	13	1,016

PPW, posterior pharyngeal wall; NOS, not otherwise specified; SCC, squamous cell carcinoma; W/D, well differentiated; M/D, moderately differentiated; P/D, poorly differentiated; NK, non-keratinizing

HPV-positive oropharyngeal squamous cell carcinomas have a propensity to originate from the inner crypts rather than the surface (Fig. 1-5). Histologically, they are typified by the presence of monotonous tumor cells exhibiting limited cytoplasm, arranged in nests, islands, and ribbons, without the characteristic formation of keratin pearls (Fig. 1-6). Table 1-4 presents the rates of positivity for HPV, p16, and the Epstein-Barr virus (EBV) in oropharyngeal SCCs tested at AMC, categorized by subsite. Specifically, HPV, p16, and EBV were detected in 74%, 79%, and 5% of cases, respectively. Importantly, it is worth highlighting that in subsites such as the soft palate, posterior pharyngeal wall, tonsillar pillar, and uvula—locations characterized by relatively sparse lymphoid tissue—the positivity rates for HPV and p16 were comparatively low. This observation implies that the lymphoid microenvironment may play a significant role in facilitating HPV infection and persistence.

Among the 389 cases tested for both HPV and p16, a total of 29 out of 306 p16-positive cases (9%) were HPV-negative, while 5 out of 282 HPV-positive cases (2%) were p16-negative. HPV typing was conducted in 309 cases, revealing the presence of HPV type 16 in 256 cases, type 35 in 15 cases, type 58 in 14 cases, type 18 in 6 cases, and types 31, 33, 39, 45, 53, 56, and 59 in various frequencies.

Table 1-4. Positive rates of HPV, p16, and EBV of oropharyngeal squamous cell carcinomas according to subsites

	Subsites	Palatine tonsil	Base of tongue	Soft palate	Vallecula	PPW	Lateral wall	Tonsillar pillar	Uvula	NOS	Total
HPV	Positive	274	46	3	4		1	1	1	1	331 (74%)
	Negative	74	20	11		3	1	5	1	3	118
p16	Positive	334	52	3	3		1	1	1	2	397 (79%)
	Negative	52	24	12	2	5	3	6	1	4	109
EBV	Positive	3	1	1							5 (5%)
	Negative	71	18	3	1	4		1		2	100

PPW, posterior pharyngeal wall; NOS, not otherwise specified; HPV, human papillomavirus; EBV, Epstein-Barr virus

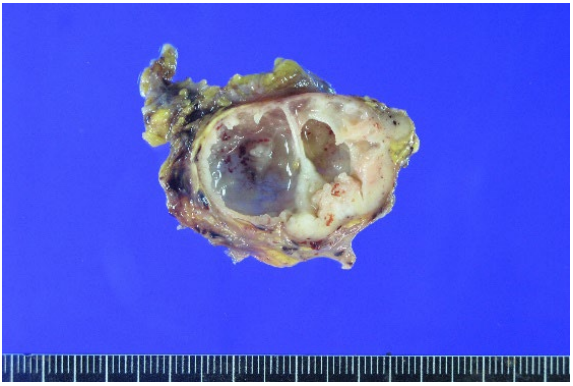

Fig. 1-5. Gross feature of squamous cell carcinoma of the palatine tonsil. Tumor is subepithelially located, and shows an expansile yellowish white cut surface with cystic changes.

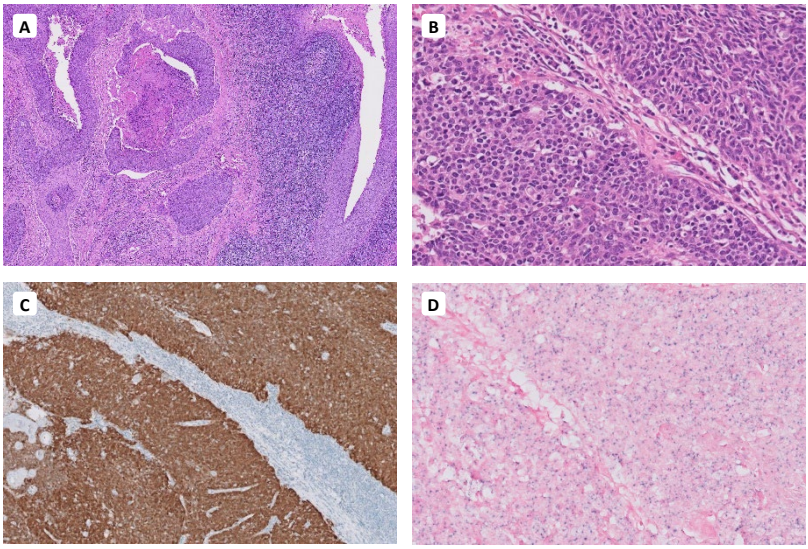

Fig. 1-6. Squamous cell carcinoma of the palatine tonsil. A. Non-keratinizing squamous cell carcinoma is involving the tonsillar crypts. B. Tumor cells are monotonous with little cytoplasms. C. Tumor cells show diffuse positivity for p16 on immunohistochemistry (IHC). D. Tumor cells show positive nuclear signals for high-risk human papillomavirus (HPV) on *in situ* hybridization (ISH).

1.3. Squamous cell carcinoma of larynx

The distribution and subtypes of laryngeal squamous cell carcinomas (SCCs) are presented in Table 1-5. The glottis was the predominant subsite, accounting for 57% of cases (Fig. 1-7A). This was followed by the supraglottis (24%) and the transglottis (12%). A significant majority of laryngeal SCCs (87%) exhibited either well or moderately differentiated histology. Notably, the glottic location was marked by the prevalence of the well-differentiated subtype (Fig. 1-8).

Table 1-5. Subtypes and distribution of laryngeal squamous cell carcinomas

Subsites / Subtypes	Glottis	Supraglottis	Transglottis	Infraglottis	NOS	Total
SCC, W/D	312	37	33	2	21	405
SCC, M/D	419	223	116	14	28	800
SCC, P/D	14	45	13	5	4	81
SCC, NOS	34	24	6	1	9	74
Spindle cell SCC	8	1	1	1		11
Basaloid SCC	1	7	1		1	10
Papillary SCC	1					1
VC	1		1			2
Total	790	337	171	23	63	1,384

NOS, not otherwise specified; SCC, squamous cell carcinoma; W/D, well differentiated; M/D, moderately differentiated; P/D, poorly differentiated; VC, verrucous carcinoma

The larynx exhibits a covering of either squamous or respiratory epithelium, contingent upon the specific subsite, and squamous cell carcinoma originating from squamous epithelium can arise from epithelial dysplasia and carcinoma *in situ*. The 2022 WHO Classification delineates both a 2-tiered and a 3-tiered classification for laryngeal epithelial dysplasia as follows: low-grade dysplasia characterized by architectural and cytologic changes occupying the lower half of the epithelium; high-grade dysplasia involving changes affecting more than the lower half of the epithelium; and carcinoma *in situ* marked by changes spanning the entire thickness of the epithelium. The latter two categories can be combined for a simplified 2-tiered classification. In conjunction with architectural and cytologic changes, the application of immunohistochemistry (IHC) for p53 and ki-67 has proven valuable in distinguishing between low-grade and high-grade dysplasia as we reported in 2023 (Fig. 1-9).

Spindle cell SCC, manifesting as an intraluminal protruding mass within the larynx (Fig. 1-7B), constitutes another variant. Histologically, it is characterized by the predominance of spindle cells displaying marked atypia (Fig. 1-10). In the larynx, the diagnosis of spindle cell SCC can be established with or without immunohistochemical positivity for cytokeratin (CK), unless conclusive evidence points to a distinct sarcoma subtype. Despite its anaplastic histology, the prognosis of spindle cell SCC is akin to

that of conventional SCC due to its protruding growth pattern and low T stage.

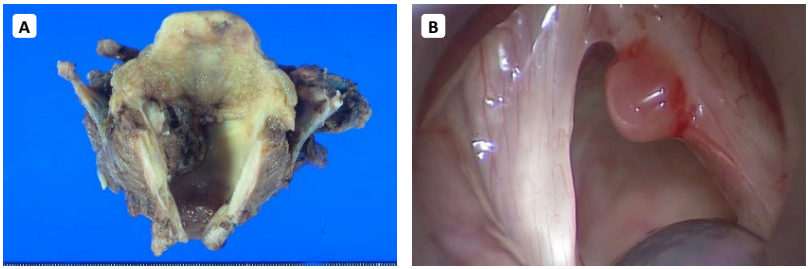

Fig. 1-7. Gross features of squamous cell carcinomas of the larynx. A. Ulceroinfiltrating tumor is involving the left transglottic area. B. Spindle cell squamous cell carcinoma is presenting as a polypoid mass on the right vocal cord.

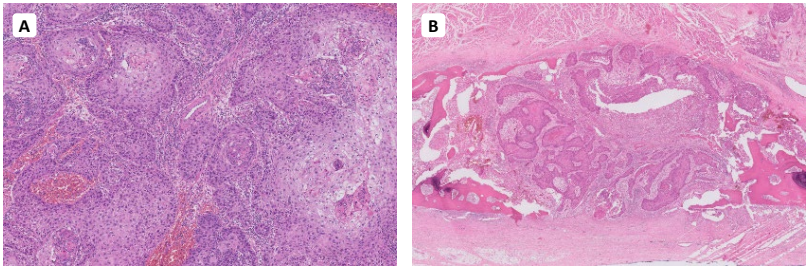

Fig. 1-8. Squamous cell carcinoma of the larynx. A. Tumor shows moderate differentiation with focal keratinization. B. Tumor is invading the ossified thyroid cartilage.

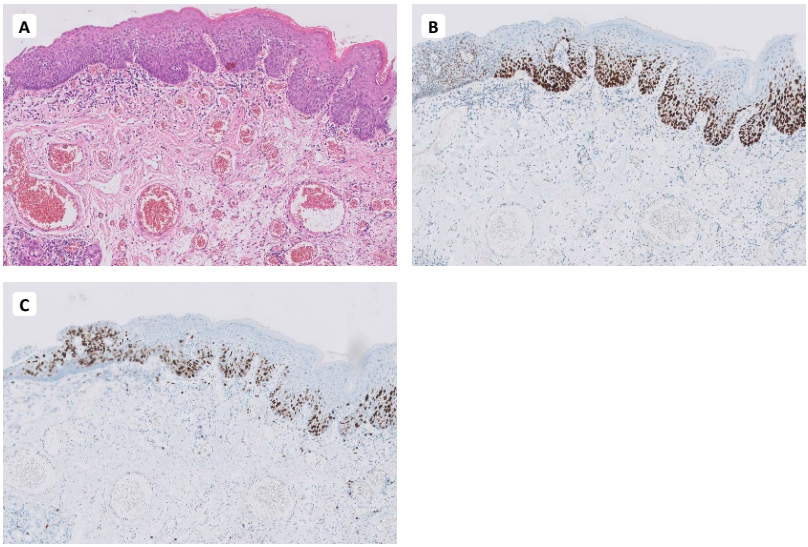

Fig. 1-9. High-grade dysplasia of the laryngeal epithelium. A. Intraepithelial cells show atypia and loss of polarity involving more than lower half of the epithelial thickness. B. p53 overexpression is observed in more than lower half of the epithelium on IHC. C. ki-67 labeling is increased up to more than lower half of the epithelium on IHC.

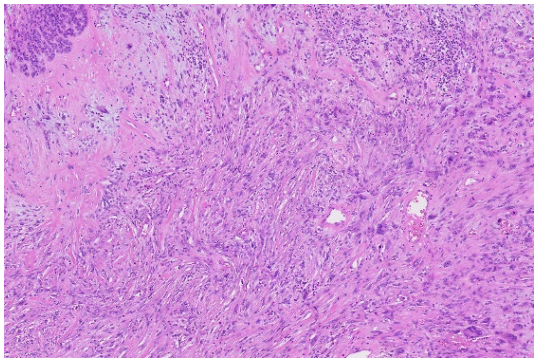

Fig. 1-10. Spindle cell squamous cell carcinoma of the larynx. Tumor is mostly composed of anaplastic spindle cells.

1.4. Squamous cell carcinoma of hypopharynx

An overview of the distribution and subtypes of hypopharyngeal squamous cell carcinomas (SCCs) is encapsulated within Table 1-6. The pyriform sinus was the prevailing subsite, accounting for 67% of cases (Fig. 1-11A), trailed by the posterior wall of the hypopharynx, constituting 12% of cases. It is noteworthy that hypopharyngeal SCC located on the posterior wall was not infrequently accompanied by synchronous or metachronous esophageal SCC. Within the hypopharynx, instances of well-differentiated SCC were relatively uncommon, while the poorly differentiated subtype accounted for 16% of cases (Fig. 1-12).

Table 1-6. Subtypes and distribution of hypopharyngeal squamous cell carcinomas

Subsites Subtypes	Pyriform sinus	PWH	Lateral wall	Postcricoid	AEF	Entire	PEJ	NOS	Total
SCC, W/D	37	5	8	2	1	1	1	3	58
SCC, M/D	267	53	12	20	15	8	4	19	398
SCC, P/D	68	11	5	6	6		2	3	101
Basaloid SCC	12	5	1					1	19
Spindle cell SCC	4		1						5
SCC, NOS	47	4	5	1				7	64
Total	435	78	32	29	22	9	7	33	645

PWH, posterior wall of hypopharynx; AEF, aryepiglottic fold; PEJ, pharyngoesophageal junction; NOS, not otherwise specified; SCC, squamous cell carcinoma; W/D, well differentiated; M/D, moderately differentiated; P/D, poorly differentiated

Basaloid SCC, a distinctive subtype, frequently involves the hypopharynx and is characterized by nests of basaloid cells with limited cytoplasm, varying in size. Noteworthy histological features include the presence of comedonecrosis, a cribriform pattern, peripheral palisading, and abundant basement membrane material. The principal basaloid components do not exhibit squamous differentiation, while there is a frequent association with squamous cell carcinoma *in situ* of the overlying epithelium (Fig. 1-12). Additionally, the presence of glandular formation, a sarcomatoid component, or a small cell carcinoma component can be observed, implying an origin from multipotential cells, as reported in our prior work. Basaloid

SCC typically presents as a protruding mass (Fig. 1-11B) and demonstrates a prognosis similar to that of conventional SCC.

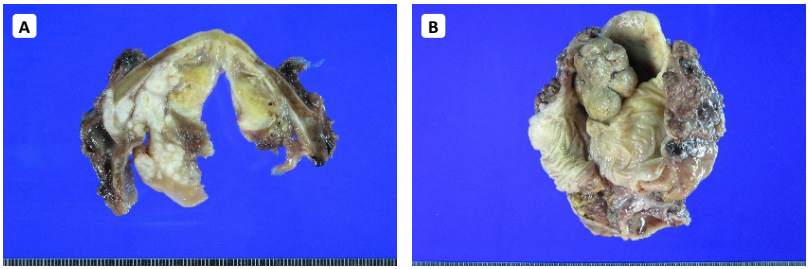

Fig. 1-11. Gross features of squamous cell carcinomas of the hypopharynx. A. Tumor in the left pyriform sinus is invading the paraglottic space and thyroid cartilage. B. A basaloid squamous cell carcinoma presents as a well demarcated protruding mass involving the left pyriform sinus and aryepiglottic fold.

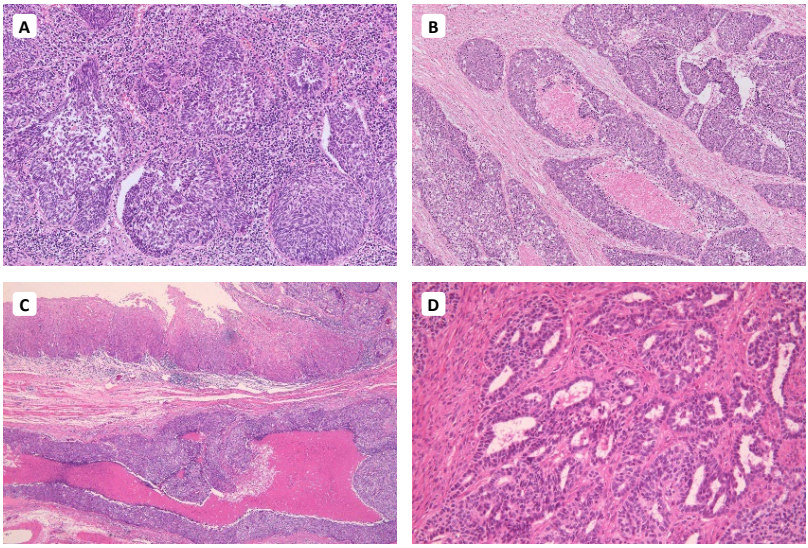

Fig. 1-12. Squamous cell carcinoma of the hypopharynx. A. Poorly differentiated squamous cell carcinoma with little squamous differentiation. B. Basaloid squamous cell carcinoma consists of lobules of basaloid cells with a peripheral palisading and comedonecrosis. C. Squamous cell carcinoma *in situ* of the overlying epithelium coexists with underlying basaloid squamous cell carcinoma. D. Glandular differentiation is noted in a basaloid squamous cell carcinoma.

1.5. Squamous cell carcinoma of sinonasal tract

The subtypes and distribution within sinonasal squamous cell carcinomas (SCCs) are shown in Table 1-7. Given that over half of the cases involved multiple subsites, the determination of location was predicated on the epicenter as identified through radiological observations. Subtypes were subsequently re-categorized into keratinizing SCC and non-keratinizing SCC in accordance with the current WHO Classification. The maxillary sinus was identified as the predominant subsite, accounting for 52% of cases (Fig. 1-13), followed by the nasal cavity at 34%. Within the spectrum of sinonasal SCCs, keratinizing and non-keratinizing subtypes constituted 56% and 35%, respectively.

Table 1-7. Subtypes and distribution of sinonasal squamous cell carcinomas

Subtypes \ Subsites	Nasal cavity	Maxillary sinus	Ethmoid sinus	Sphenoid sinus	Frontal sinus	Entire	Total
SCC, K	54	90	10	2	4		160
SCC, NK	36	43	10	7	4	2	102
Papillary SCC	3	3					6
Spindle cell SCC		5		1			6
Basaloid SCC	1	3					4
VC	1						1
SCC, NOS	3	5	1				9
Total	98	149	21	10	8	2	288

SCC, squamous cell carcinoma; K, keratinizing; NK, non-keratinizing; VC, verrucous carcinoma; NOS, not otherwise specified

Non-keratinizing SCC is characterized by the presence of expansive ribbons composed of immature squamous cells exhibiting pushing borders (Fig. 1-14). Although HPV has been implicated as a potential risk factor for sinonasal SCC, the current dataset did not contain HPV-positive cases due to insufficient testing. A notable observation from the data is that among the 288 cases of sinonasal SCC, a substantial 24% (70 cases) exhibited a concurrent presence of inverted papillomas or a prior diagnosis of such lesions. This suggests the potential malignant transformation of inverted papillomas at higher rates than reported 2~20%. The subtypes and distribution patterns of these cases are detailed in Table 1-8. This

transformation is often associated with high-risk HPV infections, smoking, and the presence of keratinizing histology (Fig. 1-14).

Table 1-8. Subtypes and distribution of sinonasal squamous cell carcinomas associated with inverted papilloma

Subtypes \ Subsites	Nasal cavity	Maxillary sinus	Ethmoid sinus	Sphenoid sinus	Frontal sinus	Entire	Total
SCC, K	16	19	3				38
SCC, NK	10	15	1		1	1	28
Papillary SCC		1					1
Basaloid SCC		1					1
SCC, NOS	2						2
Total	28	36	4	0	1	1	70

SCC, squamous cell carcinoma; K, keratinizing; NK, non-keratinizing; NOS, not otherwise specified

Papillary SCC affects the sinonasal tract and is characterized by a papillary growth pattern comprised of non-keratinizing carcinoma cells enveloping fibrovascular cores (Fig. 1-14). The inherently lower invasiveness of this subtype contributes to a more favorable prognosis compared to that of conventional SCC.

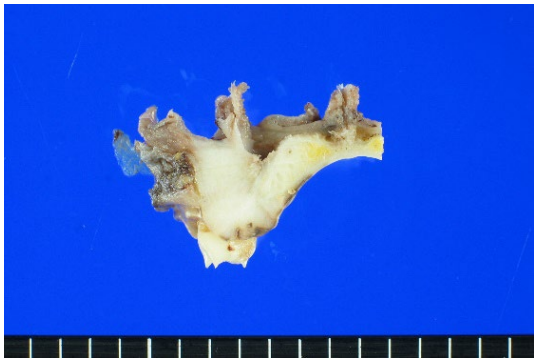

Fig. 1-13. Gross feature of squamous cell carcinoma of the maxillary sinus. Tumor is invading the maxilla bone with a yellowish white solid cur surface.

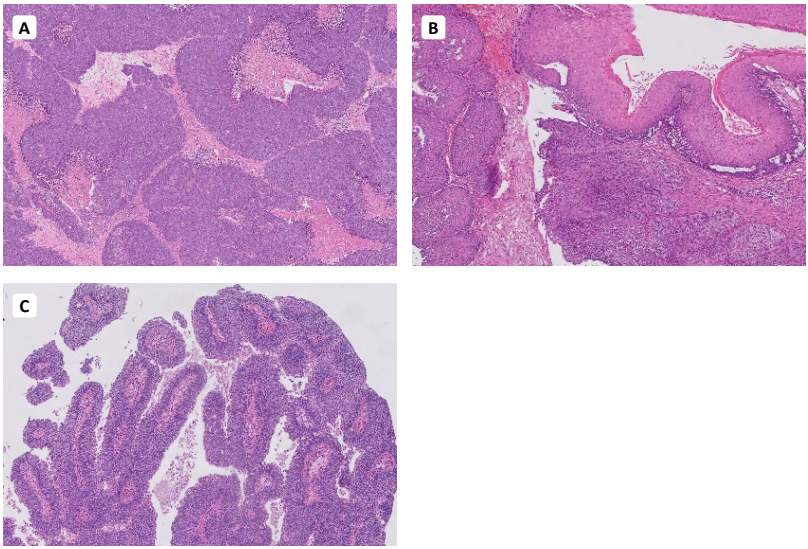

Fig. 1-14. Squamous cell carcinoma of the sinonasal tract. A. Sinonasal non-keratinizing squamous cell carcinoma consists of lobules of immature squamous cells with pushing borders. B. Keratinizing squamous cell carcinoma arising from an inverted papilloma (left side). C. Papillary squamous cell carcinoma shows papillary growth of atypical non-keratinizing squamous cells around fibrovascular cores.

1.6. Squamous cell carcinoma of nasopharynx

Nasopharyngeal squamous cell carcinoma (SCC) is classified similarly to sinonasal SCC, into non-keratinizing SCC and keratinizing SCC subtypes. The non-keratinizing SCC subtype can be further categorized into undifferentiated and differentiated subtypes, although they do not exhibit clinical distinctions. The undifferentiated subtype is histologically characterized by syncytial aggregates of undifferentiated cells, displaying indistinct cell membranes, scanty cytoplasm, vesicular nuclei, prominent nucleoli, and coexistence with lymphocytes. Conversely, the differentiated subtype comprises cases with increased stratification, lower nuclear-to-cytoplasmic ratio, less prominent nucleoli, and discernible cell borders (Fig. 1-15). Both subtypes are equally associated with the Epstein-Barr virus (EBV), with a higher prevalence in endemic regions such as southern China. The detection rates of EBV in nasopharyngeal SCC at AMC are summarized in Table 1-9, wherein 95% of non-keratinizing SCC and 21% of keratinizing

SCC cases were EBV-positive (Fig. 1-15). In a 2012 report, we noted slight differences in EBV positivity between undifferentiated and differentiated subtypes (90% vs. 84%).

Table 1-9. Positive rates of Epstein-Barr virus of nasopharyngeal squamous cell carcinomas according to subtypes

Subtypes	EBV-positive	EBV-negative	NA	Total
SCC, NK	267	15	366	648
SCC, K	3	11	29	43
Basaloid SCC		1	4	5
Spindle cell SCC	1			1
SCC, NOS		1	13	14
Total	271 (91%)	28 (9%)	412	711

EBV, Epstein-Barr virus; NA, not assessed; SCC, squamous cell carcinoma; NK, non-keratinizing; K, keratinizing; NOS, not otherwise specified

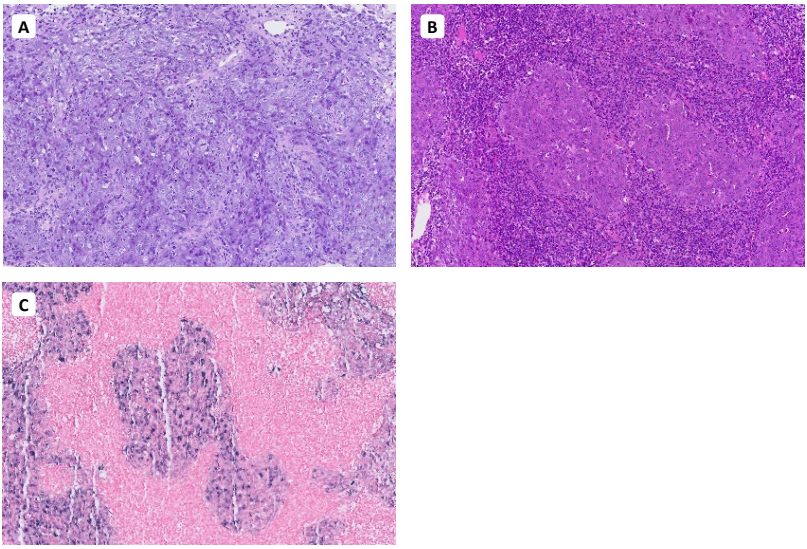

Fig. 1-15. Squamous cell carcinoma of the nasopharynx. A. Undifferentiated subtype of nasopharyngeal non-keratinizing squamous cell carcinoma is composed of syncytial aggregates of atypical cells mixed with lymphocytes. Tumor cells have vesicular nuclei, prominent nucleoli, and indistinct cell borders. B. Differentiated subtype of nasopharyngeal non-keratinizing squamous cell carcinoma shows more defined groups of carcinoma cells. C. Tumor cells harbor Epstein-Barr virus on ISH.

1.7. Squamous cell carcinoma of salivary gland

Primary squamous cell carcinomas (SCCs) arising within the salivary gland are rare, necessitating the meticulous exclusion of metastatic origins for an accurate diagnosis. In our series, eighteen cases of primary SCC were documented, with 13 cases occurring in the parotid glands and 5 cases in the submandibular glands. The patients, comprising 15 males and 3 females, exhibited ages ranging from 53 to 84 years, with a mean age of 66.4 years. Histological observations reflected conventional features, although they were distinguished by a pronounced desmoplastic reaction and peritumoral inflammation as reported in 2020. Another notable discovery from the study was the identification of androgen receptor expression in a subset of cases, suggesting a potential relationship with salivary duct carcinoma (Fig. 1-16).

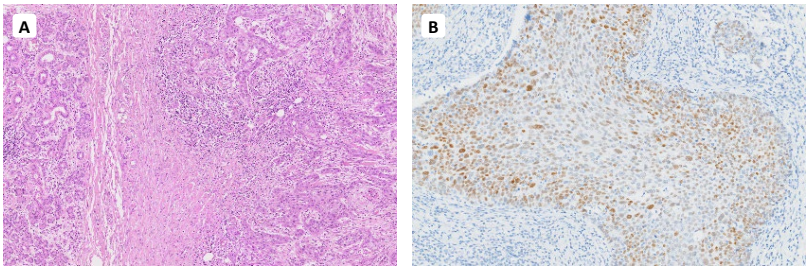

Fig. 1-16. Squamous cell carcinoma of the salivary gland. A. Moderately differentiated squamous cell carcinoma is located within the parotid gland. B. Tumor cells are positive for androgen receptor IHC, suggesting a relationship with salivary duct carcinomas.

1.8. Squamous cell carcinoma of eye

The distribution and subtypes of ocular squamous cell carcinomas (SCCs) are outlined in Table 1-10. These cases were identified in a cohort comprising 18 males and 9 females, with ages spanning from 24 to 96 years (mean age: 63.1 years).

Table 1-10. Subtypes and distribution of ocular squamous cell carcinomas

Subsites / Subtypes	Eyelid	Bulbar conjunctiva	Nasolacrimal duct	Total
SCC, W/D	5	3		8
SCC, M/D	7	4	2	13
SCC, P/D	4			4
SCC, NOS	1		1	2
Total	17	7	3	27

SCC, squamous cell carcinoma; W/D, well differentiated; M/D, moderately differentiated; P/D, poorly differentiated; NOS, not otherwise specified

Squamous cell carcinoma of the bulbar conjunctiva is an exceedingly rare occurrence, characterized by geographic disparities that exhibit a higher prevalence in the southern hemisphere compared to the northern hemisphere. Emerging evidence points to HPV as a significant risk factor, particularly among AIDS patients in Africa. In the Asian context, there is a reported female predominance; however, the current dataset encompasses 6 male and 1 female patient, ranging in ages from 58 to 86 years.

Conjunctival SCC typically manifests as a distinct, elevated lesion, often situated on the limbus (Fig. 1-17), exhibiting a well to moderately differentiated SCC pattern (Fig. 1-18). A subset of conjunctival SCC is believed to originate from conjunctival squamous intraepithelial neoplasia (CSIN). The grading system for CSIN in the 2023 WHO Classification, which classifies it as mild, moderate, severe, and carcinoma *in situ*, is advisable to be reconsidered for a 2-tier system, akin to SCC in other head and neck sites. The utilization of immunohistochemistry for p53 and ki-67 is recommended for precise grading and prognostication. CSIN is also associated with HPV infections (Fig. 1-19), and while it predominantly affects the limbus of the eye, some epidemiological evidence suggests that not all CSIN cases are precursors of SCC.